J Mater Sci: Mater Electron (2011) 22:776–780
DOI 10.1007/s10854-010-0210-z

Structure, microwave dielectric and optical properties of $Ln_{2/3}Gd_{1/3}TiNbO_6$ (Ln=Ce, Pr, Nd and Sm) ceramics

Annamma John · Shyla Joseph · K. M. Manu · J. K. Thomas · Sam Solomon

Received: 16 June 2010 / Accepted: 26 August 2010 / Published online: 17 September 2010

Abstract The $Ln_{2/3}Gd_{1/3}TiNbO_6$ ceramic compositions are prepared through the solid state ceramic route. The compositions are calcined at 1250 °C and sintered in the range 1350–1435 °C. Structural analysis of the materials is done using X-ray diffraction analysis and vibrational spectroscopy. Surface morphology is examined by Scanning Electron Microscopy. Microwave dielectric properties such as dielectric constant (ε_r), quality factor (Q) and temperature coefficient of resonant frequency (T_f) are measured using cavity resonator method. The compositions have ε_r in between 46 and 41.8 and T_f in between +52 and +25 ppm/°C. By the substitution of Gd, the T_f is reduced considerably with a slight decrease in dielectric constant. Cerium based composition had additional reflections other than that of aeschynite structure. For Pr, Nd and Sm based systems, solid solutions were formed. UV visible spectrum of the representative composition is recorded and the band gap energy is estimated. Photoluminescence spectra of the samples are recorded and the transitions causing emissions are identified. The materials are suitable for microwave and optoelectronic applications.

A. John (✉) · S. Joseph · S. Solomon
Department of physics, St. John's College, Anchal, Kerala 691306, India
e-mail: j_annamma@yahoo.com

K. M. Manu
Fine ceramics materials and minerals Division, NIIST, Thiruvananthapuram, Kerala 695019, India

J. K. Thomas
Departmentof Physics, Mar Ivanios College, Thiruvananthapuram, Kerala 695015, India

1 Introduction

The advancement in microwave communication resulted in an increased demand for new materials suitable for microwave applications [1]. Dielectric Resonators (DR), the ceramic puck used for microwave communication have the advantage of more miniaturization, high quality factor than other techniques like transmission lines, micro strips and cavities, low cost and can easily be coupled to microwave integrated circuits [2]. Widespread research is going on in the field of DR as they have high dielectric constant (ε_r), high quality factor (Q) and small variation of resonant frequency with respect to temperature (T_f) [3]. It is interesting to note that most of the DR with good dielectric properties are complex oxides of titanium, niobium and tantalum. Komkov et al. [4] and Qi et al. [5] have reported that $RETiNbO_6$ compounds with lanthanide of atomic numbers in the range 57–63 have orthorhombic aeschynite structure and those in the range 64–71 have orthorhombic euxenite structure. As per the report by Sebastian et al. [6] the aeschynite $RETiNbO_6$ materials have positive T_f with high dielectric constant while euxenite compounds have negative T_f with a lower dielectric constant. Surendran et al. [7] have reported a similar observation in the case of $RETiTaO_6$ ceramics also. It is possible to optimize the microwave dielectric properties of these ceramics by preparing suitable solid solutions and composites of aeschynite and euxenites. Solomon et al. [8] and Surendran et al. [9] reported that by making suitable solid solutions of both aeschynite and euxenite structures, it is possible to get compositions having low T_f and desirable microwave dielectric properties. Oishi et al. [10] have reported the microwave dielectric properties and crystal structure of $Sm(Nb_{1-x}Ta_x)(Ti_{1-y}Zr_y)O_6$ ceramics. Recently Kumar et al. [11] and Joseph et al. [12] reported the effect of

yttrium substitution for Nd on $NdTiTaO_6$ ceramics and $NdTiNbO_6$ ceramics and obtained near zero temperature coefficient of resonant frequency (T_f) along with good dielectric properties. Raman scattering studies to explain the structure and microwave dielectric properties of this type materials have also become significant in recent years [13–15]. Jacob et al. [16] reported the photoluminescence and dielectric properties of $LnTiTaO_6$ (Ln=Ce, Pr and Sm) polycrystals. In the present work, we report the synthesis, structural analysis, microwave and the optical properties of $Ln_{2/3}Gd_{1/3}TiNbO_6$ where Ln=Ce, Pr, Nd and Sm.

2 Experimental

The compositions $Ln_{2/3}Gd_{1/3}TiNbO_6$, where Ln=Ce, Pr, Nd and Sm, abbreviated as CGTN, PGTN, NGTN and SGTN respectively, are prepared through the conventional solid-state route. The high purity oxides (>99%)of CeO_2, Pr_2O_{11},Nd_2O_3,Sm_2O_3,TiO_2,Nb_2O_5 and Gd_2O_3 are used. Conventional solid state ceramic route is used to prepare polycrystalline samples. Samples are calcined at 1,250 °C, pellitized and sintered in the range 1,350–1,435 °C. The densities of well- polished samples are calculated using Archimedes method. Powdered samples are used for X-ray diffraction (Philips Expert Pro) studies using Cu–Kα radiation. The cell parameters are calculated using the least square method and the theoretical densities are determined. Polished sample is thermally etched at 1,300 °C and is used for Scanning Electron Microscopy (SEM) (JEOL JSM 5610 LV). The dielectric properties of the samples are measured in the microwave frequency region using the cavity resonator method with the help of network analyzer. The temperature coefficient of resonant frequency is also measured over a range of temperature 30–70 °C. The FT-Raman spectra of the compounds are recorded over the range 50–1,000/cm using a Bruker RFS 100/s FT Raman spectrometer using an Nd:YAG laser source lasing at 1,064 nm and a Ge diode detector. The resolution of the instrument is 4 cm^{-1} and the power level used is 25 mW. The photoluminescence spectra of the samples were also taken and the emission lines are identified. The absorption spectra of a sample were also recorded and the bandgap energy was estimated. The photoluminescence spectra are taken using Perkin Elmer LS 55 Xenon Lamp Spectrometer. The UV spectrum is taken using The Double beam UV–Vis Spectrometer and the bandgap is identified.

3 Results and discussion

Figure 1a shows the XRD pattern of CGTN. It is a mixture of $CeTiNbO_6$ (ICDD file 15-864), $GdTiNbO_6$ (ICDD file 27-221), TiO_2 (ICDD file 21-1276) and Nb_2O_5 (ICDD file 30-873). The reflections of $CeTiNbO_6$ and $GdTiNbO_6$ are indexed and the other reflections are marked as (*) in the pattern. Hence it is clear that CGTN does not form an exact solid solution and is nearly a composite.

Figure 1b shows the XRD patterns of PGTN, NGTN and SGTN ceramics. The reflections of these compounds are similar to that of aeschynite structure. That is exact solid solutions are formed in these compounds. The microwave dielectric properties, the lattice parameters and theoretical densities of $Ln_{2/3}Gd_{1/3}TiNbO_6$ where Ln=Ce, Pr, Nd and Sm, are given in Table 1. As Ln moves from left to right in the periodic table, there is a gradual decrease in ε_r and T_f and a gradual increase in experimental (ρ_{exp}) and theoretical (ρ_{the}) densities. ε_r varies from 54 to 45 and T_f from +67 to +50 for pure $LnTiNbO_6$ [6, 12]. In the Gadolinium (Gd) substituted sample ε_r varies from 46 to 41.8 and T_f

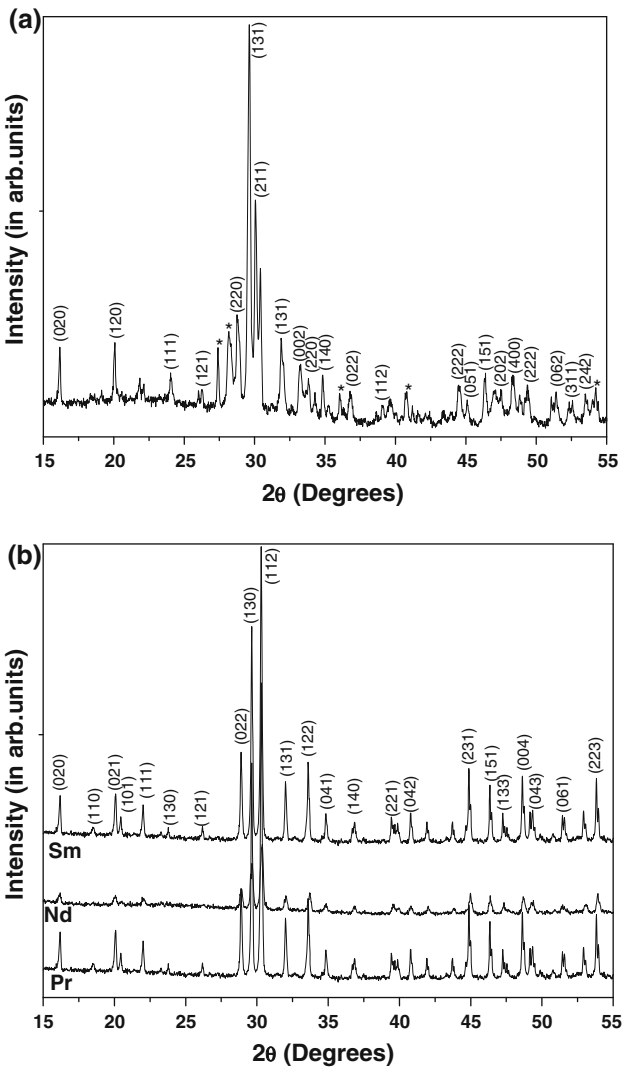

Fig. 1 **a** X-ray diffraction patterns of of CGTN ceramic. **b** X-ray diffraction patterns of of PGTN, NGTN and SGTN ceramics

Table 1 Microwave dielectric properties of $Ln_{2/3}Gd_{1/3}TiNbO_6$ (Ln=Ce, Pr, Nd and Sm)

Lanthanide	ε_r	f (GHz)	τ_f (ppm/°C)	$Q_u$xf (GHz)	Lattice parameters(A°)			ρ_{the} (g/cc)	ρ_{exp} (g/cc)
					a	b	c		
Ce	46.1	3.44925	+52.64	5,070	*	*	*	*	5.4655
Pr	44.2	3.56668	+45.98	12,975	5.27	11.01	7.50	5.842	5.5342
Nd	42.7	3.64693	+38.58	6,830	5.30	11.01	7.47	5.877	5.5389
Sm	41.8	3.70406	+25.48	7,500	5.27	11.01	7.50	5.938	5.6435

* Not calculated since it is a composite

The SEM picture of PGTN is shown in Fig. 3. It shows that the sample is well sintered with minimum porosity. The particle size ranges from 2 to 10 μm

from +52 to +25. Therefore by the substitution of Gd, the T_f is reduced considerably with a slight decrease in dielectric constant.

Figures 2a and 3 shows the variation in εr and τf with respect to the average ionic radii of Ln and Gd. There is a gradual increase in εr and τf with the increase in average ionic radii. Figure 2b shows that the experimental density and theoretical density decrease with increase in the average ionic radii of lanthanides. These variations are in agreement with the earlier reports [9–11].

UV absorption spectra of the compound NGTN is given in Fig. 4. As neodymium is a lanthanide, it absorbs photons in the UV and visible regions. The transitions responsible

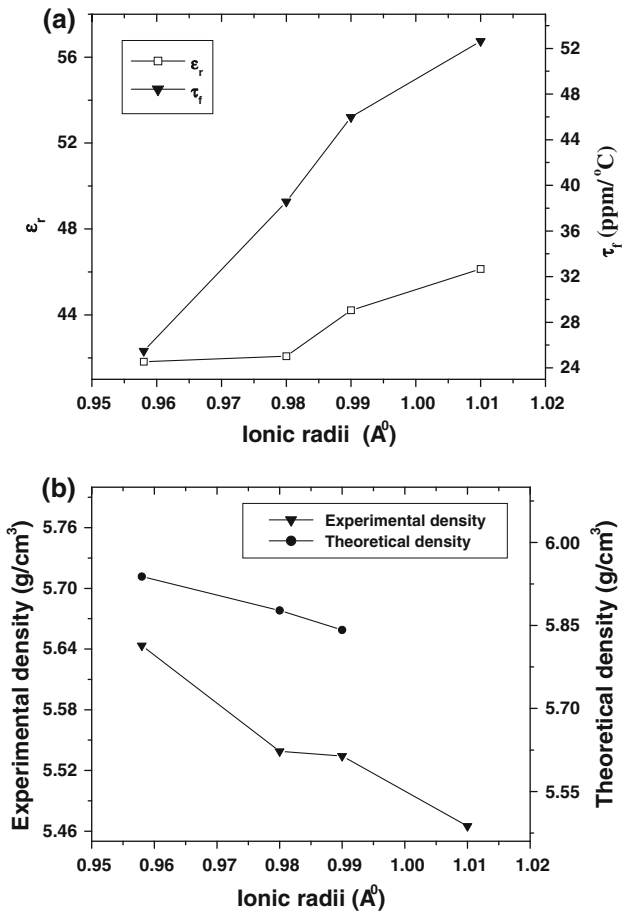

Fig. 2 **a** Variation in ε_r and τ_f with respect to the average ionic radii of lanthanides. **b** Variation of experimental density and theoretical density with the average ionic radii of lanthanides

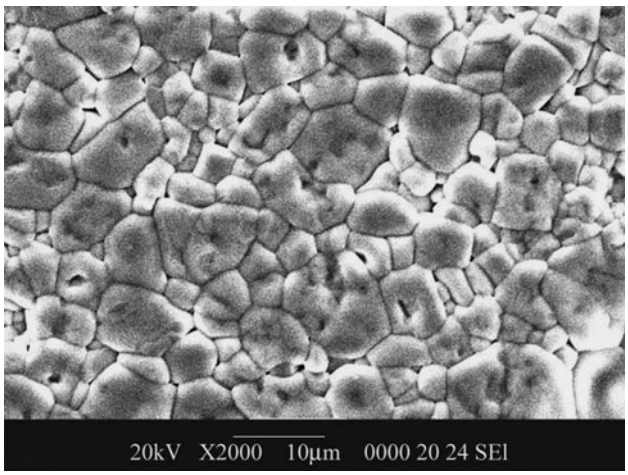

Fig. 3 SEM image of PGTN ceramic

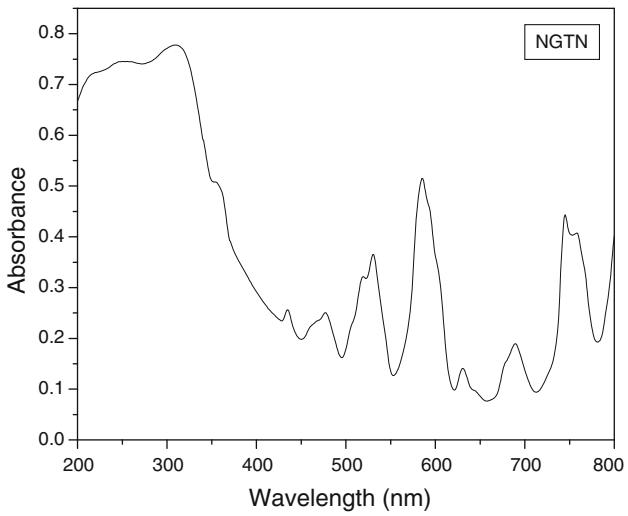

Fig. 4 UV absorption spectrum of NGTN ceramic

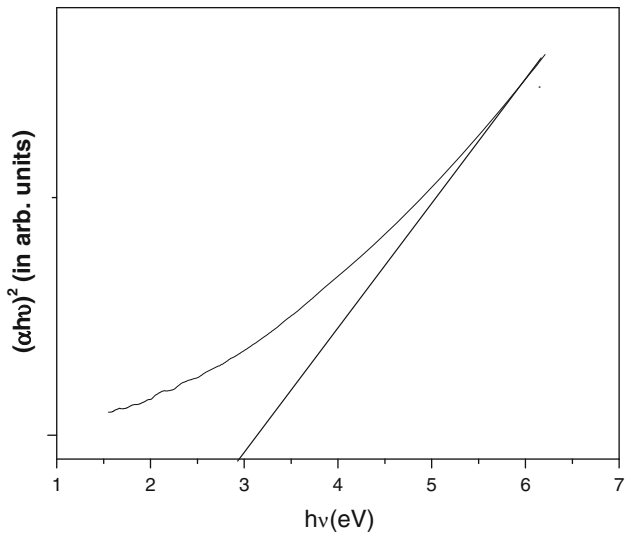

Fig. 5 Graph to estimate the band gap energy of NGTN

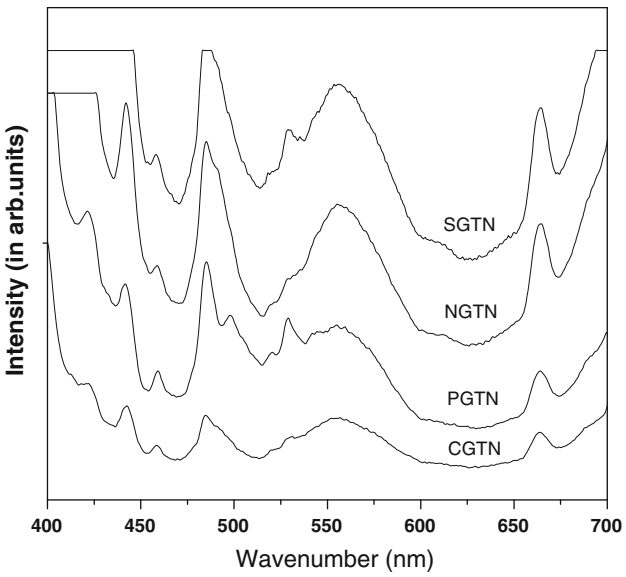

Fig. 6 PL emission spectrum of Ln2/3Gd1/3TiNbO6 ceramics

for this absorption appear to involve the various energy levels of 4f electrons. These inner orbitals are largely screened from external influences by electrons occupying orbital with higher principal quantum numbers. As a consequence its spectra consist of narrow, well defined and characteristic peaks. Spectral characteristics of gadolinium involve electronic transitions among the various energy levels of 4d orbital. The absorption bands are often broad and strongly influenced by chemical environmental factors [17]. The material has absorption bands in the wavelength range 500–800 nm. Average particle size is calculated using Scherrer formula. A graph (Fig. 5) was plotted between $(\alpha h\upsilon)^2$ and $h\upsilon$ (in eV), where α is the absorption coefficient. The value of the band gap is estimated by extrapolating the steep portion of the graph to zero absorbance. This tangential line coincides with the X axis at 2.9 eV and the corresponding wavelength is 417.6 Å.

Powdered samples are subjected to photoluminescence studies. Scanning was done in the range 400–700 nm and was excited at 370 nm. The spectra obtained are given in Fig. 6. The transitions are identified on the basis of the data book by Payling and Larkins [18]. The photoluminescence spectrum of CGTN shows emission lines at 423, 443, 460, 557 and 664 nm. The two characteristic peaks at wavelengths 423 and 443 nm are due to the transitions $^9F_4^0$-$^5H_4$ and $^9F_4^0$-$^7G_4$ of Gadolinium atom and that at 460 nm is due to the transition of $^4F_5^4$-$^4F_{4.5}^*$ of Niobium atom. The line at 557 nm is due to the transition $^5I_5^{00}$-A_5^0 of Cerium atom. The line at 664 nm is due to the transition of $^3F_2$-$^5G_4^0$ of Titanium atom.

The PL spectrum of PGTN shows emission lines at 422, 442, 497, 522 and 664 nm. The line observed at 422 nm is due to the transition $^9p_3$-$^0A_4^0$ due to Gadolinium atom and that observed at 442 nm is due to the transition $^4I_{15/2}^0$-$^0A_{13/2}$ of Praseodymium. The line at 497 nm is due to the transition $^4G_5^4$-$^4F_5^3$ of Niobium. The lines at 422 and 664 nm are due to the transition $^3F_4$-$^3F_4^0$ and $^3F_2$-$^5G_4^0$ respectively of Titanium.

The PL spectrum of NGTN show emission lines at 442, 460, 485, 559 and 664 nm. The lines observed at 442 and 485 nm are due to transition $^5I_6^0$-A_6^0 and $^5I_4$-$^0A_3^0$ due to Neodymium atom respectively and that at 460 nm is due to the transitions $^7D_5^0$-$^7G_5$ of Gadolinium atoms. The line at 559 nm is due to the transition of $^4D_5^2$-$^4D_5^1$ of Niobium atom and that at 664 nm is due to the transition of $^3F_2$-$^5G_4^0$ of Titanium.

For SGTN the PL spectrum shows emission lines at 460, 485, 529, 664 and 696 nm. The emission lines observed at 484 nm are due to the transition $^7F_4$-$^5F_4^0$ of Samarium. The line at 460 nm is due to the transition $^9F_5^0$-$^7H_6$ of Gadolinium. The line at 529 and 664 nm are due to the transitions of $^5F_{2S}$-$^3P_2^0$ and $^3F_2$-$^5G_4^0$ respectively of Titanium. The line observed at 696 nm is due to the transition $^4G_5^2$-$^6D_5^2$ of Niobium.

Figure 7 shows the Raman spectra of CGTN and SGTN and their spectral data and band assignments are given in Table 2. According to Qi et al. [5] $RETiNbO_6$ with RE ions of atomic number in the range 57–63 have orthorhombic aeschynite structure and those in the range 64–71 have orthorhombic euxenite structure. Paschoal et al. [14] have reported the Raman scattering study of the microwave dielectric system $RETiTaO_6$ for 15 different lanthanide of isovalance ions. The Raman spectra of CGTN and SGTN are found to be similar to that reported by Paschoal et al. for the aeschynite structure. The spectra are exactly similar to that reported for $CeTiTaO_6$ and $GdTiTaO_6$ both belonging to the aeschynite structure. The CGTN has most

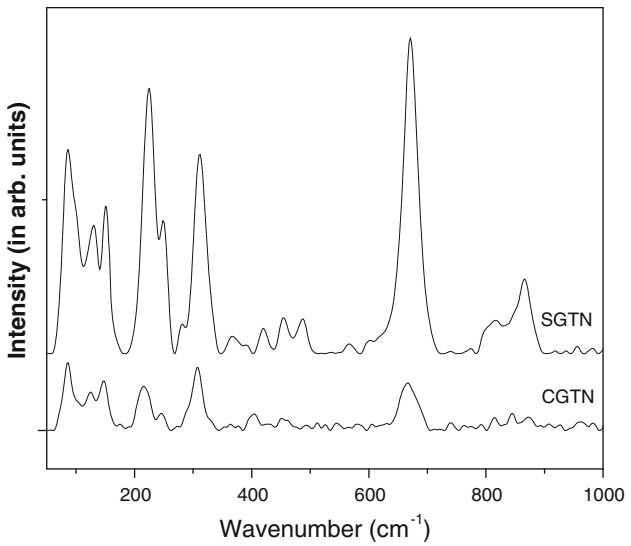

Fig. 7 Raman spectra of CGTN and SGTN ceramics

Table 2 Raman spectral data and band assignment of CGTN and SGTN

CGTN	SGTN
872 vw	865 m
845 m	
815 w	814 w
739 vw	
666 s	671 vs
	566 vvw
545 vw	
512 vw	
	487 w
451 m	454 w
404 m	420 w
307 vs	311 s
245 m	249 m
215 s	225 s
147 s	151 m
125 s	130 m
86 vs	86 s

of the bands similar to that of aeschynite structure. However the bands in the Nb compounds have slightly lower intensity than that associated with Ta compounds due to the mass difference between the two. To conclude, both CGTN and SGTN have aeschynite orthorhombic structure.

4 Conclusion

Solid solutions of $Ln_{2/3}Gd_{1/3}TiNbO_6$ (Ln=Ce, Pr, Nd and Sm) ceramics were prepared through the conventional solid state route. The materials were calcined at 1,250 °C and sintered at optimized temperature in the range 1,350–1,435 °C. The structure of the system was analyzed by XRD and vibrational spectroscopic studies. Cerium based composition had additional reflections other than that of aeschynite structure. For Pr, Nd and Sm based systems, solid solutions were formed. The sinterability and surface morphology were analyzed using SEM. Microwave dielectric properties were measured using the cavity resonator method. Thermal stability is achieved without much variation in dielectric constant of $LnTiNbO_6$ ceramics. The UV spectra were studied and the bandgap energy is estimated. Photoluminescence spectra were analyzed and the corresponding transitions are identified.

References

1. M. Reaney, D. Iddles, J. Am. Ceram. Soc. **89**, 2063 (2006)
2. W. Wersing, Curr. Opin. Solid. State Mater. Sci. **1**, 715–731 (1996)
3. R.J. Cava, J. Mater. Chem. **11**, 54–62 (2001)
4. I. Komkov, Dokl. Acad. Nauk **148**, 1182 (1963)
5. X. Qi, R. Illingworth, H.G. Gallagher, T.P.J. Han, B. Henderson, Potential laser gain media with stoichiometric formula $RETiNbO_6$. J. Cryst. Growth **160**, 111–118 (1996)
6. M.T. Sebastian, S. Solomon, R. Ratheesh, J. George, P. Mohanan, J. Am. Ceram. Soc. **84**(7), 1487–1489 (2001)
7. K.P. Surendran, P. Mohanan, M.T. Sebastian, J. Eur. Ceram. Soc. **23**, 2489–2495 (2003)
8. S. Solomon, M. Kumar, K.P. Surendran, M.T. Sebastian, P. Mohanan, Mater. Chem. Phys. **67**, 291 (2001)
9. K.P. Surendran, M.R. Varma, P. Mohanan, M.T. Sebastian, J. Am. Ceram. Soc. **86**, 1695 (2003)
10. T. Oishi, A. Kan, H. Ohsato, H. Ogawa, J. Eur. Ceram Soc. **26**, 2075–2079 (2006)
11. H.P. Kumar, J.K. Thomas, M.R. Varma, S. Solomon, J. Alloys. Compd. **455**, 475 (2008)
12. S. Joseph, M.K. Suresh, J.K. Thomas, A. John, S. Solomon, Int. J. Appl. Ceram. Technol. **7**, 129–134 (2009)
13. R. Ratheesh, H. Sreemoolanathan, S. Solomon, P.R. Ratheesh, H. Sreemoolanathan, M.T. Sebastian, Vibrational analysis of $Ba_{5-x}Sr_xNb_4O_{15}$ dielectric ceramics. J. Solid State Chem. **131**, 2–8 (1997)
14. C.W.A. Paschoal, R.L. Moreira, C. Fantini, M.A. Pimenta, K.P. Surendran, M.T. Sebastian, Raman scattering study of $RETiTaO_6$ dielectric ceramics. J. Eur. Ceram. Soc. **23**, 2661–2666 (2003)
15. M.-Y. Chen, C.-T. Chia, I.-N. Lin, L.-J. Lin, C.-W. Ahn, S. Nahm, Microwave properties of $Ba(Mg_{1/3}Ta_{2/3})O_3$, $Ba(Mg_{1/3}Nb_{2/3})O_3$ and $Ba(Co_{1/3}Nb_{2/3})O_3$ ceramics revealed by Raman scattering. J. Eur. Ceram. Soc. **26**, 1965–1968 (2006)
16. L. Jacob, H. Padmakumar, K.G. Gopchandran, J.K. Thomas, S. Solomon, Photoluminescence and dielectric properties of $LnTiTaO_6$ (Ln=Ce,Pr,Sm) polycrystals. J. Mater. Sci. Mater. Electron. **18**(8), 831–835 (2007)
17. D.A. Skoog, F.J. Holler, T.A. Nieman, *Principle of Instrumental Analysis*, 5th edn. (Harcourt Asia Pte Ltd., Singapore, 1998), pp. 335–337, 355–358
18. R. Payling, P. Larkins (Wiley Verlag, New York, June 2000)